CHALMERS
UNIVERSITY OF TECHNOLOGY

Single-photodiode per polarization receiver with signal-signal beat interference suppression through heterodyne detection

Citation for the original published paper (version of record):
Corcoran, W., Foo, B., Lowery, A. (2018). Single-photodiode per polarization receiver with signal-signal beat interference suppression
through heterodyne detection. Optics Express, 26(3): 3075-3086.
http://dx.doi.org/10.1364/OE.26.003075

Research Article | Vol. 26, No. 3 | 5 Feb 2018 | OPTICS EXPRESS 3075
Optics EXPRESS

Single-photodiode per polarization receiver with signal-signal beat interference suppression through heterodyne detection

Bill Corcoran,[1,2,*] Benjamin Foo,[1,3] and Arthur J. Lowery[1,2]

[1] *Electro-Photonics Laboratory, Dept. Electrical and Computer Systems Engineering, Monash University, VIC 3800, Australia*
[2] *Centre for Ultrahigh-bandwidth Devices for Optical Systems (CUDOS), Australia*
[3] *Currently with: Photonics Lab, Dept. Microtechnology and Nanoscience (MC2), Chalmers University of Technology, Gothenburg SE-412 96, Sweden*
[*] *bill.corcoran@monash.edu*

Abstract: We show that a simplified, single-photodiode per polarization heterodyne receiver is able to directly suppress signal-signal beat interference (SSBI), without the need for cancellation in the digital domain. We characterize performance degradation due to SSBI, and show that a strong LO in the receiver can mitigate SSBI. Transmission of 400 Gb/s-class signals is shown over single fiber spans of up to 160 km, and over field-deployed metropolitan area fiber. These results indicate that a single photodiode can be used to receive complex optical signals in high speed fiber systems without the need for SSBI cancellation in the digital domain.

OCIS codes: (060.1660) Coherent communications; (060.2840) Heterodyne.

References and links

1. Cisco, "Cisco Visual Networking Index," https://www.cisco.com/c/en/us/solutions/service-provider/visual-networking-index-vni/index.html.
2. D. Che, A. Li, X. Chen, Q. Hu, Y. Wang, and W. Shieh, "Stokes vector direct detection for linear complex optical channels," J. Lightwave Technol. **33**, 678–684 (2015).
3. M. Chagnon, M. Morsy-Osman, and D. V. Plant, "Half-terabit single carrier direct detect transceiver, formats and DSP: Analysis and demonstration," J. Lightwave Technol., doi: 10.1109/JLT.2017.2769623.
4. K. Szczerba, P. Westbergh, M. Karlsson, P. A. Andrekson, and A. Larsson, "70 Gbps 4-PAM and 56 Gbps 8-PAM using an 850 nm VCSEL," in "2014 The European Conference on Optical Communication (ECOC)," (2014), pp. 1–3.
5. R. I. Killey, P. M. Watts, V. Mikhailov, M. Glick, and P. Bayvel, "Electronic dispersion compensation by signal predistortion using digital processing and a dual-drive Mach-Zehnder modulator," IEEE Photonics Technol. Lett. **17**, 714–716 (2005).
6. R. Rodes, M. Wieckowski, T. T. Pham, J. B. Jensen, J. Turkiewicz, J. Siuzdak, and I. T. Monroy, "Carrierless amplitude phase modulation of VCSEL with 4 bit/s/Hz spectral efficiency for use in WDM-PON," Opt. Express **19**, 26551–26556 (2011).
7. J. D. Ingham, R. V. Penty, I. H. White, and D. G. Cunningham, "Carrierless amplitude and phase modulation for low-cost, high-spectral-efficiency optical datacommunication links," in "Conference on Lasers and Electro-Optics 2010," (Optical Society of America, 2010), p. CThC5.
8. A. J. Lowery, L. Du, and J. Armstrong, "Orthogonal frequency division multiplexing for adaptive dispersion compensation in long haul WDM systems," in "Optical Fiber Communication Conference and Exposition and The National Fiber Optic Engineers Conference," (Optical Society of America, 2006), p. PDP39.
9. A. J. Lowery, "Comparisons of spectrally-enhanced asymmetrically-clipped optical OFDM systems," Opt. Express **24**, 3950–3966 (2016).
10. A. S. Karar and J. C. Cartledge, "Generation and detection of a 56 Gb/s signal using a DML and half-cycle 16-QAM Nyquist-SCM," IEEE Photonics Technol. Lett. **25**, 757–760 (2013).
11. M. S. Erkilinç, S. Pachnicke, H. Griesser, B. C. Thomsen, P. Bayvel, and R. I. Killey, "Performance comparison of single-sideband direct detection Nyquist-subcarrier modulation and OFDM," J. Lightwave Technol. **33**, 2038–2046 (2015).
12. J. Armstrong and A. J. Lowery, "Power efficient optical OFDM," Electron. Lett. **42**, 370–372 (2006).
13. N. Fernando, Y. Hong, and E. Viterbo, "Flip-OFDM for unipolar communication systems," IEEE Trans. Comm. **60**, 3726–3733 (2012).

#315206 https://doi.org/10.1364/OE.26.003075
Journal © 2017 Received 7 Dec 2017; revised 14 Jan 2018; accepted 16 Jan 2018; published 29 Jan 2018

Optics EXPRESS

14. W.-R. Peng, X. Wu, K.-M. Feng, V. R. Arbab, B. Shamee, J.-Y. Yang, L. C. Christen, A. E. Willner, and S. Chi, "Spectrally efficient direct-detected OFDM transmission employing an iterative estimation and cancellation technique," Opt. Express **17**, 9099–9111 (2009).
15. Z. Li, M. S. Erkılınç, K. Shi, E. Sillekens, L. Galdino, B. C. Thomsen, P. Bayvel, and R. I. Killey, "SSBI mitigation and the Kramers-Kronig scheme in single-sideband direct-detection transmission with receiver-based electronic dispersion compensation," J. Lightwave Technol. **35**, 1887–1893 (2017).
16. A. Mecozzi, C. Antonelli, and M. Shtaif, "Kramers–Kronig coherent receiver," Optica **3**, 1220–1227 (2016).
17. Z. Li, M. Erkılınç, K. Shi, E. Sillekens, L. Galdino, B. Thomsen, P. Bayvel, and R. Killey, "Joint optimisation of resampling rate and carrier-to-signal power ratio in direct-detection Kramers-Kronig receivers," in "European Conference on Optical Communications," (2017), p. W.2.D.3.
18. X. Chen, C. Antonelli, S. Chandrasekhar, G. Raybon, J. Sinsky, A. Mecozzi, M. Shtaif, and P. Winzer, "218-Gb/s single-wavelength, single-polarization, single-photodiode transmission over 125-km of standard singlemode fiber using Kramers-Kronig detection," in "Optical Fiber Communication Conference Postdeadline Papers," (Optical Society of America, 2017), p. Th5B.6.
19. S. Le, K. Schuh, M. Chagnon, F. Buchali, R. Dischler, V. Aref, H. Buelow, and K. Engenhardt, "8x256Gbps virtual-carrier assisted WDM direct-detection transmission over a single span of 200km," in "European Conference on Optical Communications Postdeadline Papers," (2017), p. Th.PDP.B.1.
20. X. Chen, C. Antonelli, S. Chandrasekhar, G. Raybon, A. Mecozzi, M. Shtaif, and P. Winzer, "4 x 240 Gb/s dense WDM and PDM Kramers-Kronig detection with 125-km SSMF transmission," in "European Conference on Optical Communications," (2017), p. W.2.D.4.
21. Y. Zhu, K. Zou, X. Ruan, and F. Zhang, "Single carrier 400G transmission with single-ended heterodyne detection," IEEE Photonics Technol. Lett. **29**, 1788–1791 (2017).
22. X. Li, Z. Dong, J. Yu, J. Yu, and N. Chi, "Heterodyne coherent detection of WDM PDM-QPSK signals with spectral efficiency of 4b/s/Hz," Opt. Express **21**, 8808–8814 (2013).
23. T. M. Hoang, M. Y. S. Sowailem, M. Morsy-Osman, M. Chagnon, D. Patel, S. Paquet, C. Paquet, I. Woods, O. Liboiron-Ladouceur, and D. Plant, "Transmission of 344 Gb/s 16-QAM using a simplified coherent receiver based on single-ended detection," IEEE Photonics J. **8**, 1–8 (2016).
24. A. Carena, V. Curri, P. Poggiolini, and F. Forghieri, "Dynamic range of single-ended detection receivers for 100GE coherent PM-QPSK," IEEE Photonics Technol. Lett. **20**, 1281–1283 (2008).
25. T. Okoshi, K. Emura, K. Kikuchi, and R. T. Kesten, "Computation of bit-error rate of various heterodyne and coherent-type optical communication schemes," J. Opt. Comm. **2**, 89–96 (1981).
26. B. L. Kasper, C. A. Burrus, J. R. Talman, and K. L. Hall, "Balanced dual-detector receiver for optical heterodyne communication at Gbit/s rates," Electron. Lett. **22**, 413–415 (1986).
27. G. Nicholson, "Probability of error for optical heterodyne DPSK system with quantum phase noise," Electron. Lett. **20**, 1005–1007 (1984).
28. T. M. F. Alves and A. V. T. Cartaxo, "Virtual carrier-assisted direct-detection MB-OFDM next-generation ultra-dense metro networks limited by laser phase noise," J. Lightwave Technol. **33**, 4093–4100 (2015).
29. B. J. Schmidt, Z. Zan, L. B. Du, and A. J. Lowery, "100 Gbit/s transmission using single-band direct-detection optical OFDM," in "Optical Fiber Communication Conference and National Fiber Optic Engineers Conference," (Optical Society of America, 2009), p. PDPC3.
30. G. R. Walker, N. G. Walker, R. C. Steele, M. J. Creaner, and M. C. Brain, "Erbium-doped fiber amplifier cascade for multichannel coherent optical transmission," J. Lightwave Technol. **9**, 182–193 (1991).
31. S. Yamashita and T. Okoshi, "Suppression of beat noise from optical amplifiers using coherent receivers," J. Lightwave Technol. **12**, 1029–1035 (1994).
32. C. R. Doerr, P. J. Winzer, S. Chandrasekhar, M. Rasras, M. P. Earnshaw, J. S. Weiner, D. M. Gill, and Y.-K. Chen, "Monolithic silicon coherent receiver," in "Optical Fiber Communication Conference and National Fiber Optic Engineers Conference," (Optical Society of America, 2009), p. PDPB2.
33. C. R. Doerr, L. Zhang, and P. J. Winzer, "Monolithic InP multi-wavelength coherent receiver," in "National Fiber Optic Engineers Conference," (Optical Society of America, 2010), p. PDPB1.
34. S. B. Estrella, L. A. Johansson, M. L. Masanovic, J. A. Thomas, and J. S. Barton, "Widely tunable compact monolithically integrated photonic coherent receiver," IEEE Photonics Technol. Lett. **24**, 365–367 (2012).

1. Introduction

As the amount of data carried in metropolitan/regional area networks and data-center interconnects is growing at a faster rate than for long-haul fiber networks [1], there is significant research focus on developing simplified receiver systems more suited for these 'short-haul' systems. In long-haul fiber systems, a standard receiver for use in polarization multiplexed systems carrying complex optical data uses a local oscillator (LO) laser, two polarization-diverse 90^o optical hybrids, 4 balanced photodiode pairs and 4 high-speed analogue-to-digital converters (ADCs). Such a receiver requires precision optical components, precise matching of path lengths in both the

Optics EXPRESS

optical and electrical domain, and a low-linewidth laser. For receivers in short-haul systems, these requirements are commonly viewed as unacceptable in terms of cost, complexity and overall size.

There are several receiver systems that aim simply to remove the requirement for an LO laser while retaining optical hybrids for signal mixing, including Stokes-vector direct detection [2] and Mueller-vector direct detection [3]. While these schemes allow for complex modulation and polarization multiplexing, they still require four ADCs to digitize their outputs, and precision opto-electronic engineering. At the other extreme, pulse amplitude modulation (PAM) using direct detection on a single photodiode requires only a single ADC and photodiode (e.g. [4]), but removes the ability to use polarization multiplexing and phase encoding. Moreover, electronic chromatic dispersion compensation is problematic for intensity-only detection, only particularly effective if the dispersion map is known *a-priori* (e.g. [5]). Alternately, the link dispersion can be managed with optical dispersion compensation modules, although this adds extra loss.

To regain the ability to receive a complex optical signal, and thus allow for both phase and amplitude modulation and electronic dispersion compensation, the addition of a virtual carrier that is transmitted along with the signal enables several different approaches to modulation with the same basic receiver hardware as for PAM. These include carrier-less amplitude-and-phase (CAP) [6, 7], multiple variants of orthogonal frequency division multiplexing (OFDM) [8] (also see review in [9]), and Nyquist sub-carrier modulation [10]. By measuring the beat term between the signal and the virtual carrier, phase and amplitude information can be extracted from a single photodiode. However, in this case, signal-signal beating becomes an interference term that distorts the received signal. Solutions to this problem have been to include a guard-band between the virtual carrier and signal bands, so that the signal-signal beat interference (SSBI) terms fall in a separate frequency range to the signal-carrier beat [8, 11], and selective sub-carrier encoding in OFDM systems [12, 13]. For these approaches, spectral efficiency is reduced, practically limiting channel data rates.

To regain this lost spectral efficiency, various SSBI compensation approaches have been devised, based on SSBI as a deterministic product of sent data. Several approaches have been proposed, some specific to formats like OFDM ([9] and references therein), others more generally applicable [14, 15]. Specifically, [15] showed that SSBI cancellation based on Kramers-Kronig detection [16] provides superior performance over a range of SSBI cancellation schemes. The Kramers-Kronig detection scheme relies on the use of a strong carrier to ensure minimum-phase detection of the complex signal, and a signal processing algorithm that requires a high rate (>2 samples-per-symbol) re-sampling and interpolation [17]. Kramers-Kronig processing has enabled demonstrations of high data rate receivers using a single photodiode [18, 19], and is currently the state-of-the-art method for high data rate, single-photodiode receivers. However, the need for a strong carrier limits the sensitivity of these formats, as the required carrier-to-signal power ratio (CSPR) limits signal-to-noise ratio for a given optical signal-to-noise ratio (OSNR) [17]. This results in a limit to the CSPR available before the system performance degrades significantly.

While the inclusion of a virtual carrier and SSBI cancellation allows for spectrally efficient QAM modulation, the single-photodiode receivers proposed to date require a LO to allow for polarization multiplexing [16, 20, 21]. Recently, receivers with a simplified optical front-end using a single-photodiode per polarization were proposed [20, 21], using Kramers-Kronig digital processing for SSBI cancellation after detection.

However, the inclusion of a LO can allow for SSBI cancellation within the optical front-end by using balanced photodetection in a heterodyne receiver, removing the need for digital SSBI cancellation. This has been shown to enable polarization-multiplexed, high data-rate systems [22]. However, while the balanced photodiode heterodyne system demonstrated in [22] has a less complex optical front-end than an intradyne receiver, using balanced photodiodes still require precision path length matching of optical components. While balanced photodiodes were removed in [23], similar path length matching restrictions apply, while also requiring SSBI cancellation,

Optics EXPRESS

as expected (see [24]).

A powerful LO, however, may allow for SSBI cancellation in the optical front end without the need for precise path-length matching. The addition of a LO enables a higher maximum useful CSPR by removing the need to transmit a strong, or indeed any, virtual optical carrier. As the optical carrier is introduced locally, there is no OSNR penalty for using a high CSPR, as opposed to SSBI cancellation techniques that rely on transmitting a significant amount of power along with the signal as a virtual carrier [9, 14–19]. Moreover, as was commonly noted in coherent optical communication investigations decades earlier (e.g. [25–27]), a higher LO power allows for a lower power signal to be detected with the same received electrical signal waveform amplitude. As such, a higher LO power allows for a lower signal power. This in turn means that while the wanted signal-carrier beat term can be kept constant, the lower signal power reduces the magnitude of the unwanted signal-signal beat term significantly. This then suggests that the addition of a LO to a single photodiode detection system should enable significant reductions in the SSBI without requiring further digital signal processing.

Here we investigate the ability of a single-photodiode per polarization heterodyne receiver to provide detection of a complex optical signal without digital SSBI cancellation. We directly measure the SSBI contribution in this system with varied CSPRs, and link this to performance degradation in systems tests. We then demonstrate operation of this receiver in detecting 400 Gb/s channels, under noise loading and in single span transmission tests, including trials over field installed metropolitan-area fiber. As we do not transmit a virtual carrier, our measurements show around 5-dB benefit in using a heterodyne system in terms of required OSNR with respect to prior demonstrations of comparable Kramers-Kronig direct detection, and a single-span reach of an 8-channel, 3.2 Tb/s WDM system of 150 km over standard single-mode fiber. This demonstration suggests that high complexity digital signal processing for SSBI cancellation can be replaced with off-the-shelf components, without requiring precision engineering of signal path-lengths in the receiver.

2. Heterodyne optical detection for coherent communication systems

Heterodyne coherent detection systems use a LO that is a frequency (f_{LO}) outside of the optical bandwidth of the signal (centered at f_{sig}) that is being measured (e.g. [25–27]). As such, the real and imaginary components of the optical signal are projected onto a RF carrier on the photodetected optical waveform at a frequency $f_{het} = f_{sig} - f_{LO}$. This offset means that the real-valued photodetected waveform can convey the phase and amplitudes of the optical signal. A complex baseband electrical signal, with in-phase and quadrature components, can be obtained by mixing the photodetected signal with an oscillator of frequency f_{het} (i.e. of the form $\exp[j2\pi f_{het}t]$). This is in contrast to the intradyne coherent detection systems commonly used in long-haul fiber links, where two photodetected waveforms are required to reconstruct the complex baseband signal. Intradyne and heterodyne receivers then have fundamentally different hardware constraints, as illustrated in Fig. 1.

The basic trade-off for intradyne against heterodyne receivers is hardware complexity against component bandwidth requirements. The intradyne receiver requires, at minimum, photodetectors and ADCs with a bandwidth equal to half the baud rate of the incoming optical signal, and also needs to optically mix and measure the signal and LO beat synchronously against two different (ideally $\pi/2$ shifted) LO phase states. In contrast to this, the heterodyne system requires only one optical signal-LO mix-and-measure stage, simplifying the electro-optic front-end, but the photodetector and ADC bandwidth needs to be equal to the signal baud rate, at a minimum. In systems limited by receiver bandwidth intradyne receivers might be preferred, as intradyne systems require lower receiver E-O bandwidths than an equivalent homodyne receiver (i.e. $B/2$ vs. B in Fig. 1). However, in systems where optical front-end complexity is considered a problem, such as with short-haul links, heterodyne systems may deserve consideration. Moreover,

Optics EXPRESS

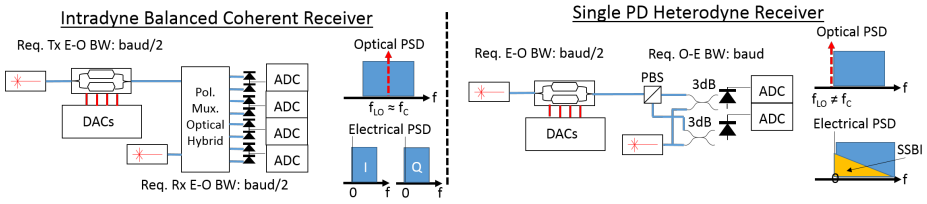

Fig. 1. Comparison on hardware requirements for a polarization diverse a) intradyne or b) heterodyne coherent optical receivers. Minimum E-O component bandwidth requirements are noted, and insets illustrate received optical and electrical spectra

heterodyne systems require the same electro-optic bandwidths as virtual carrier direct detection systems [19, 28, 29], and so can be directly compared in a fair manner.

With coherent receivers, balanced photodiodes are generally employed to remove common-mode signals. When mixing signal and LO in a 50%/50% (3-dB) optical coupler, the common signal-signal beat terms on each photodiode ideally should cancel, while the complementary signal-LO beat out of each arm of the coupler ideally should add. However, this requires a precision 50/50 split on the coupler and path-length matching between the coupler and the photodiodes down to a small fraction of a bit period. Using a single photodiode to obtain this mixing product does not require such precision, but does not cancel the SSBI [24]. However, as the ratio of signal-LO beat to signal-signal beat increases with CSPR, a high LO power can allow for significant detected signal amplitude relative to SSBI [24]. To clarify this, we can analyze the photocurrent (I_{rec}) generated in measuring a single-polarization signal in a single photodiode heterodyne receiver (as illustrated Fig. 1(b)), assuming that the signal (E_{sig}) and LO (E_{LO}) fields are co-polarized on a single photodiode:

$$I_{rec} = R_0 \times P_{rec} = R_0 \times \left(E_{sig} + E_{LO}\right)\left(E_{sig} + E_{LO}\right)^* = R_0 \times \left(P_{sig} + P_{LO} + 2\sqrt{P_{sig}}\sqrt{P_{LO}}\cos\theta\right) \tag{1}$$

where R_0 is the photodiode responsivity, P_x is denotes optical power and θ is the phase between signal and LO. The P_{LO} term is low frequency and can be DC-blocked, whereas the wanted signal×LO cross-term ($2\sqrt{P_{sig}}\sqrt{P_{LO}}\cos\theta$) can be in-band with the unwanted SSBI term (P_{sig}). As the received electrical power is proportional to the square of the photocurrent, the electrical power ratio of these two terms (assuming a uniform distribution of theta) is proportional to:

$$\frac{\left\langle I_{sig\times LO}\right\rangle^2}{\left\langle I_{sig\times sig}\right\rangle^2} = \frac{2P_{LO}}{P_{sig}} \tag{2}$$

where $\left\langle I_{sig\times LO}\right\rangle^2$ represents the signal×LO electrical signal power and $\left\langle I_{sig\times sig}\right\rangle^2$ the power of the unwanted SSBI. The above equation suggests that the signal-to-interference power ratio should scale with the CSPR. As such, a powerful LO may enable a single photodiode to be used to measure a coherent optical signal with SSBI reduced purely through the detection process.

3. Characterization of SSBI in single-photodiode heterodyne detection

To ascertain the impact of SSBI in a single-photodiode heterodyne receiver, we directly measured the spectra of the signal and interference products when the LO was frequency offset from that signal's optical carrier by over twice the signal baud rate. Figure 2(a) shows the experimental set-up. Light from an external cavity laser (ECL) is modulated using a dual-polarization InP complex Mach-Zehnder modulator (InP DP-CMZM). A 35-GHz bandwidth modulator was driven by a 33-GHz bandwidth arbitrary waveform generator (AWG) running at 90 GSa/s. In

Optics EXPRESS

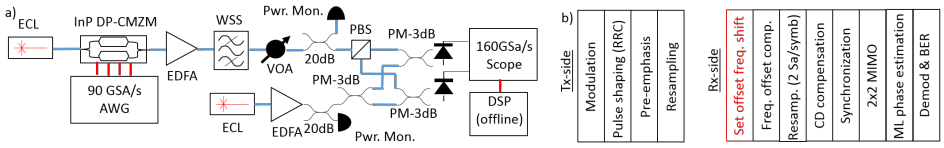

Fig. 2. a) Back-to-back set-up for characterization of SSBI against CSPR. WSS: Wavelength selective switch, PBS: Polarization beam splitter, PM-3dB: polarization maintaining 3-dB coupler. b) Transmitter- and receiver-side digital signal processing stacks. These represent common DSP flow for intradyne detection, with the exception of the (red) set value frequency shifting stage at the receive-side

this experiment, a 10-Gbd 16-QAM waveform was generated, shaped by a 10% roll-off digital root-raised cosine (RRC) filter and pre-emphasised to provide a flat optical response. The signal was amplified and the received signal power in back-to-back tests was controlled with a variable optical attenuator (VOA). The power of the LO, derived from a second ECL, was set by a power-controlled Erbium-doped fiber amplifier (EDFA), and is set to provide either 8.5 or 11.5 dBm at each photodiode. The signal and LO are injected into a single photodiode-per-polarization receiver, built from off-the-shelf polarization maintaining 3-dB couplers, a polarization beam splitter, and two 70-GHz bandwidth photodiodes. The output of the photodiodes were digitized by two 160 GSa/s, 62.5-GHz bandwidth channels of a real-time oscilloscope. The resulting waveforms were processed off-line.

The signal DSP flow at the transmitter and receiver sides is shown in Fig. 2(b). At the transmitter side, data was concatenated with a synchronization header and filtered with a 10% roll-off RRC filter with a bandwidth equal to the symbol rate, before re-sampling to match the sample rate of the AWG. At the receiver, the received signal was DC-blocked, down-shifted by a set f_{het} value, then residual frequency offset was compensated by a spectral peak search. After re-sampling to 2 Sa/symbol, chromatic dispersion compensation was applied before frame synchronization. The signal was then equalized by a blind radial decision-directed constant-modulus algorithm with taps initialized by a training-based least-means-square (LMS) pre-convergence stage. A maximum-likelihood phase estimator then reduced phase noise before demodulation and bit-error counting. We note that very similar DSP flows are commonly used for intradyne receivers, excepting the simple set frequency shift that we apply here to bring the signal down close to base-band.

In order to investigate the effect of SSBI in our system, we first set a signal-LO detuning (f_{het}) of 32 GHz, to allow for the signal-signal and signal-LO beat terms to be analyzed separately, as the SSBI term will lie around DC while the signal-LO term with lie around 32 GHz. By taking the Fourier transform of the measured waveforms, and integrating over the bands where the signal-signal and signal-LO beat lie, the ratio of signal to interference and noise (SINR) for different set CSPR values (i.e. signal to LO power ratio) is extracted. Representative measured spectra are shown in Fig. 3(a), which shows the integration windows used for signal and interference-and-noise measurement. The signal-signal beat lies within the 0-12 GHz range, as expected for a 'rectangular' RRC shaped signal at 10-Gbd, and the integrated power over this window is taken as the 'interference and noise' power. The signal-LO beat is measured in a 12 GHz bin around 32 GHz, and the integrated power over this window is taken as the signal power.

The measured SINR is plotted against CSPR in Fig. 3(b). As the 'carrier' in this set-up is the LO introduced at the receiver, the CSPR we measure is the ratio of the LO power to the signal power present at the photodiodes. The measured value of SINR increases with CSPR as expected (see Eq.(2)). In this experiment, as shown in Fig.2, the CSPR is changed by attenuating the signal for a constant LO power. This means that at high CSPR values, the received signal power is

Optics EXPRESS

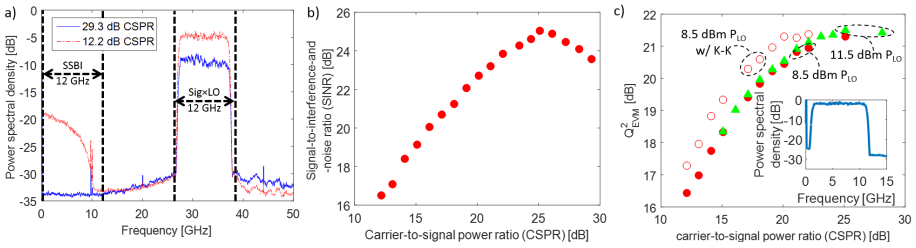

Fig. 3. Characterization of the effect of CSPR on SSBI in a single photodiode-per-polarization heterodyne receiver. a) Received electrical spectra at high and low CSPR with a 32 GHz carrier-signal detuning to spectrally resolve signal-carrier beat and signal-signal beat, b) Signal-to-interference-and-noise ratio inferred from received spectra against measured against measured carrier-to-signal power ratio, and c) received signal quality against CSPR for a 11 GHz carrier-signal detuning

reduced, toward the noise floor of the receiver. Hence, as the CSPR is increased, the SINR peaks and then gradually decreases, as the received signal power becomes comparable with the noise floor of the receiver. Moreover, the SSBI beat falls within the receiver noise floor at high CSPR (see Figs.3(a) & 3(b)), indicating that at CSPR values above 25 dB, SSBI should be negligible.

This is further supported by the trace marked by open circles in Fig. 3(c), which represent the same received waveforms as those marked by the closed circles, except that Kramers-Kronig DSP is used as the first step in the DSP flow, prior to down-sampling from the 160-GSa/s oscilloscope sampling rate to 2 Sa/s for the rest of the DSP, giving an oversampling rate of 16×. Where the signal is significantly impaired by SSBI, Kramer-Kronig reception gives a 1 dB Q^2 improvement, before saturating at around 21 dB at higher CSPR. The Kramers-Kronig DSP allows received signal quality to saturate at around 20 dB CSPR in this particular case, about a 5 dB improvement over the case without Kramers-Kronig DSP. This result seems to indicate that although the Kramers-Kronig DSP can significantly improve performance in heterodyne systems when impaired by SSBI, at very high received Q^2 there would seem to be room for improvement in SSBI cancellation, as in this experiment we would expect a constant Q2 regardless of CSPR if SSBI was fully cancelled. This may indicate that a further rigorous study, focusing on the SSBI cancellation efficacy of Kramers-Kronig DSP, is warranted.

We then decreased the signal-LO detuning to f_{het} = 6 GHz, so that the signal-LO beat of the 10% roll-off signal lies in the same band as the signal-signal beat, and measure signal quality derived from error vector magnitude (EVM) as $Q^2 = 20 \times \log_{10}(EVM)$. Figure 3(c) plots this against measured CSPR, with the LO ('carrier') power at each photodiode set to either 8.5 or 11.5 dBm. As with the SINR, the signal quality decreases with decreasing CSPR. At low CSPR, the performance is clearly limited by SSBI. We note that performance seems to be independent of the carrier power used, indicating that SSBI is the major limiting signal impairment. At higher CSPRs, signal quality asymptotes to around Q^2 =21.5 dB, and signal quality is limited by a combination of back-to-back OSNR and receiver noise. This then indicates that for CSPRs above 25 dB, SSBI has a negligible effect on signal quality on received 10Gbd signal, reflecting the direct measurement of SINR. Note that, however, as the measured signal bandwidth increases, the received SNR should decrease as the signal power is spread out over a wider received bandwidth changing the achievable asymptotic Q^2. This indicates that for higher-bandwidth signals (as considered in the next section), the optimal CSPR may be considerably lowered, as the interference power will need to be larger to start to significantly outweigh the intrinsic receiver noise.

Optics EXPRESS

4. Performance in 400-Gb/s-per-channel systems

4.1. Back-to-back characterization

We next characterize the performance of the heterodyne receiver in detecting signals designed to carry 400 Gb/s. We chose to use the same DP-16-QAM modulation with the same 10% RRC shaping as used in the prior section, but operated at symbol rates varying from 56- to 62-Gbd. We first analyze signal performance against optical noise. Figure 4(a) shows the experimental set-up for back-to-back trials with noise loading. Here, the symbol rate is changed from 56- to 60-, 61- or 62-Gbd, with a set LO offset of f_{het} = 32 GHz. The 56-Gbd rate targets channels with 7-10% FEC overheads, and the 60- to 62-GBd rates target 20% FEC overheads. This allows for net data rates ranging between 400 and 419 Gb/s (for 60-Gbd, 20% FEC and 56-Gbd, 7% FEC, respectively). Note that the optical filter in the receiver is set at 100-GHz bandwidth to emulate the function of a 100-GHz channel de-multiplexing filter, which will result in some out-of-band noise being folded into the measured signal band upon heterodyne detection.

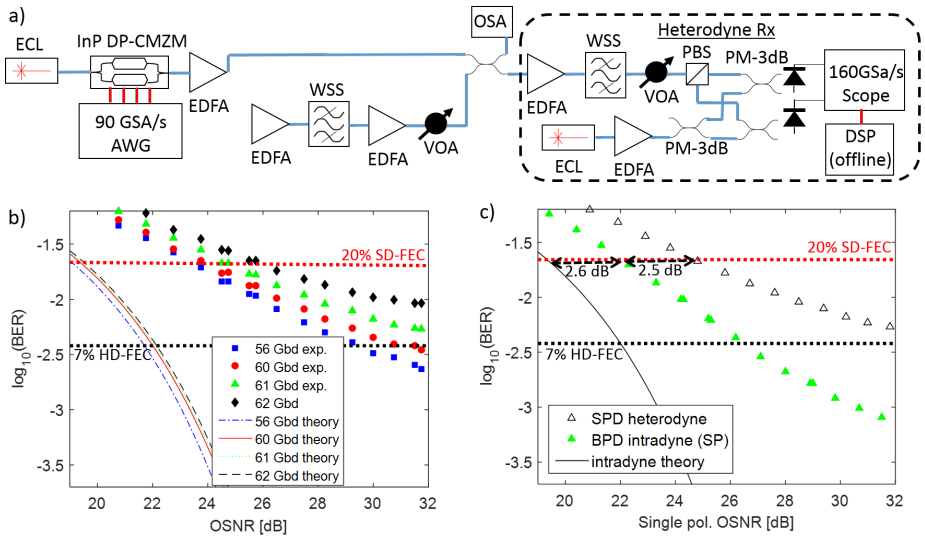

Fig. 4. a) Experimental set-up for back-to-back noise loading experiments. OSA: optical spectrum analyzer. b) Performance against received OSNR for heterodyne received signals at various symbol rates (closed points), and theoretical performance assuming intradyne coherent detection (lines). c) Measured receiver performance when detecting a 61 Gbd signal, with intradyne (closed points) receiving a single-polarization signal and (open points) heterodyne receiving a dual polarization signal.

Figure 4(b) shows measured bit-error rate against received OSNR for the range of symbol rates tested. As symbol rate increases, BER for a given OSNR decreases. Notably, the traces for 60- to 62-Gbd signals asymptote out toward significantly different error floors. Part of this effect can be attributed to the bandwidth limit of the oscilloscope used in the experiment. This has a hard cut-off anti aliasing filter that attenuates measured components significantly at frequencies above 62.5 GHz. For the 10% roll-off signals used here, this severely affects the high frequency components of the 62-Gbd signal, much less so the 60-Gbd signal. For the 56-Gbd signal, the entire signal band is comfortably accommodated in the bandwidth of the oscilloscope.

We also measure performance of the single-photodiode heterodyne system against a balanced photodiode intradyne system employing a 90^o optical hybrid. For the intradyne system, the optical paths for 'I' or 'Q' component measurement are matched to below 1 ps by the manufacturers of the separate optical hybrid and balanced 43-GHz bandwidth PDs. The remaining I/Q receiver

Optics EXPRESS

path skew is compensated manually using the in-built channel skew function of the oscilloscope to below 0.5 ps (147.0 ps skew). To make a fair comparison, we use the two available 160 GSa/s inputs to the oscilloscope, for both the heterodyne and intradyne systems. This allows for only single-polarization detection for the intradyne system. As such, only a single-polarization signal is delivered to the intradyne receiver, while the heterodyne receiver detects a polarization-multiplexed signal. To compare these two receivers, their performance is plotted against single-polarization received OSNR in Fig. 4(c). The performance of the balanced photodiode, optical hybrid intradyne receiver is clearly better than the single-photodiode per polarization heterdyne receiver, both in terms of required OSNR at the 20% SD-FEC limit indicated, and error floor indicated by the two traces. At the 20% SD-FEC limit, the implementation penalty (in terms of required OSNR) for the intradyne detection systems is 2.6 dB, with a further 2.5-dB penalty when receiving using the single-photodiode heterodyne set-up. This is consistent with the out-of-band noise sensitivity of heterodyne receivers, where LO-ASE beat is a significant noise source. For heterodyne measurement, optical noise outside of the signal band can be imaged back onto the signal upon heterodyne reception [30, 31]. In this case, as mentioned above, we use a 100-GHz bandwidth optical filter before the receiver, so some out-of-band noise is present at the receiver. With intradyne systems, only in-band LO-ASE beat noise is measured. We note that this out-of-band noise sensitivity effect may also limit the sensitivity of virtual carrier heterodyne systems [15, 18, 19].

4.2. WDM transmission

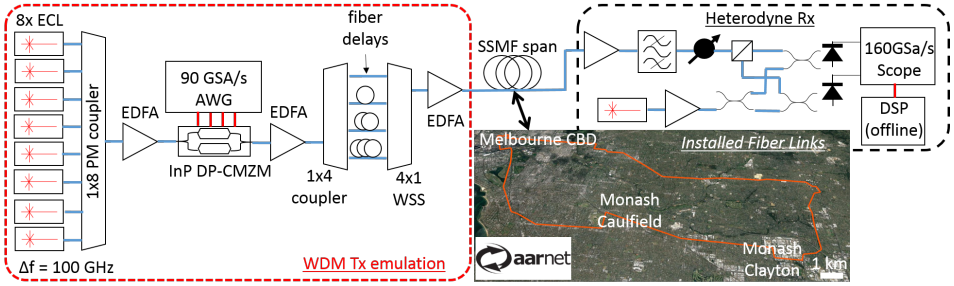

Fig. 5. Experimental set-up for 8-channel 100-GHz-grid WDM experiments. Between the emulated WDM transmitter and heterodyne receiver is placed either a lumped loss (VOA), a single span of in-lab spooled fiber, or a span of installed metropolitan dark fiber. Inset: map of the Australian Lightwave Infrastructure Research Test-bed (ALIRT), hosted by Australia's Academic and Research Network (AARNet).

We next investigated performance when receiving multiplexed signals in a WDM system. Here, the outputs of eight ECLs were separated in frequency by 100 GHz are combined in a PM 1×8 coupler, amplified to 20 dBm by a PM-EDFA before being simultaneously modulated. After the modulator, the band is passively split four ways, passed through four different lengths of SMF for temporal decorrelation, then 100/400 GHz four-way interleaved using a 1×4 wavelength selective switch to create an A-B-C-D WDM channel structure. The channel powers are equalized to within 1 dB. The experimental set-up is shown in Fig. 5. After aggregation, the eight channels are then either attenuated before reception, passed through single spans of standard single mode optical fiber (G.652.D), or through field installed, metropolitan-area fibers (see the inset of Fig. 5 for a map of the fiber routes). The total launch power in all cases was +12 dBm (+3 dBm per channel), which provided the maximum performance.

To characterize the link loss budget for our system, Fig. 6(a) shows BER of the center channel at 193.1 THz, with loss between the transmitter and pre-amplified receiver varied, for 56- and

Optics EXPRESS

61-Gbd symbol rates per channel. Up to 19-dB loss, there is little variation in the BER, as back-to-back noise dominates over noise from amplified spontaneous emission added by the receiver optical amplifier. For losses beyond this BER degrades, with the 56-Gbd signal crossing a commonly used 7% hard-decision FEC threshold at 3.8×10^{-3} for losses above 26-dB, and the 61-Gbd signal passing thorough a common 20% soft-decision FEC threshold at BER=2.2×10^{-2} for losses exceeding 30 dB.

The performance after transmission over single-spans of optical fibers with different lengths is shown in Fig. 6(b). Again, we analyzed the center channel. Here, we have concatenated different combinations of 30- and 50-km long spools of G.652.D standard single-mode fiber to vary the 'single span' distance that the signal is transmitted over. Using the indicative 7% and 20% FEC thresholds for the 56- and 61-Gbd signals respectively, we were able to achieve reaches of 130 km and 150 km respectively. Comparing the loss of these different length spans (26.6 dB and 29.6 dB) to the loss budget described in Fig. 6(a), these reaches are as expected. This indicates that chromatic dispersion is sufficiently compensated in receiver-side DSP, and that standard inter-datacenter and metropolitan area reaches are achievable for 400G channels with our simplified receiver.

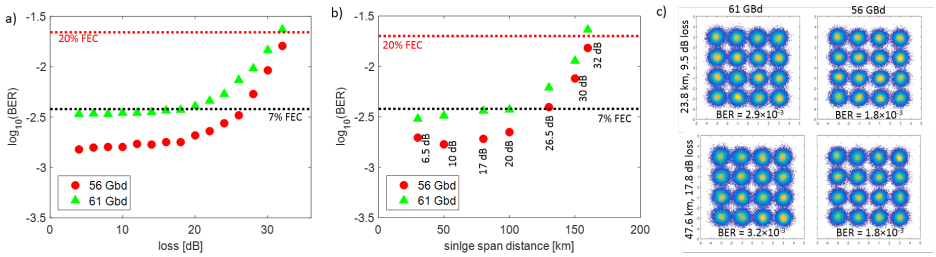

Fig. 6. Performance curves for the center (193.1 THz) channel, heterodyne received, after WDM transmission. a) BER against loss for a lumped loss only between transmitter and receiver, b) BER against transmission distance for in-lab fibers (span losses marked against points), and c) 'X'-polarization constellations and dual-pol. BER after in-field transmission.

To show that the proposed system is robust to real environmental variations and cabling issues, we next transmit over field-installed metropolitan-area dark fibers available to us through the Australian Lightwave Infrastructure Test-bed (ALIRT), provided by AARNet. These fibers consist of loop-backs between Monash University's Caulfield and Clayton campus, and a ring connecting Monash Clayton with Melbourne CBD. The Caulfield-Clayton connection that we used here consists of two fiber pairs of 23.8-km length and 8-8.5 dB loss. Fiber lengths were confirmed using optical time domain reflectometry. Signal constellations and BER after transmission through this field-trial test-bed for the center WDM channel at 193.1 THz are shown in Fig. 6(c), and BER in each case is below the 7% HD-FEC threshold. Again, similarly to the in-lab test fiber, we show a good match between span loss and performance, indicating that our system is robust to environmental fluctuations in field-installed fiber, and demonstrates that the proposed system may be deployed in existing fiber infrastructure.

5. Discussion

In this paper, we have shown a receiver that utilizes a two separate photodiodes to detect signals on two orthogonal polarizations, enabled by using a LO laser. We acknowledge that the addition of a LO in receivers for short haul applications is contentious. Here we find that a LO can be used to remove the requirement for SSBI cancellation, double capacity through polarization multiplexing and enable a simple optical front end for PM-mQAM signal detection. Moreover, as demonstrated by [20], a LO in a transceiver architecture can be re-used, even in heterodyne

Optics EXPRESS

detection. As such, the addition of a LO to single-photodiode receivers may prove to be more beneficial in terms of added capability, than it is detrimental in terms of cost.

We compare our results against published results in comparable systems using SSBI cancellation in Table 1. Published results for Kramers-Kronig receivers in systems running at similar symbol and gross data rates, required 36-dB OSNR for a pre-FEC BER of 1.7×10^{-2} on a 60-GHz wide, adaptively loaded DMT signal [18], and 32 dB OSNR for a pre-FEC BER of 1×10^{-2} with a 16-QAM, 64-Gbd signal [19]. For our 60-Gbd 16-QAM system, we require 27-dB OSNR at a pre-FEC BER of 1×10^{-2} (see Fig.4). This indicates that the use of a heterodyne reception system to suppress SSBI can operate at 5-dB lower OSNR than comparable results using Kramers-Kronig schemes [18, 19]. Comparing our results to the 16-QAM, 56-Gbd heterodyne system employing Kramers-Kronig SSBI cancellation [21], at their chosen pre-FEC rate BER threshold of 4.5×10^{-3}, the measured required OSNR is 28.5 dB. In our 56-Gbd 16-QAM heterodyne system without Kramers-Kronig reception, we show here an identical sensitivity at this BER. This indicates that a strong lLO in a single-photodiode heterodyne receiver is able to suppress SSBI, removing the need for Kramers-Kronig receiver DSP. Note that we also forgo the recursive-least squares and maximum-likelihood sequence detection stages placed after phase correction in [21]. There is a clear caveat here that there must be sufficient power available to be used as LO and as the transmit optical carrier for our scheme to be used in the architecture proposed in [20], in order to remove the need for Kramers-Kronig receiver DSP.

Table 1. Required OSNR for single-photodiode receivers when measuring signals targeting net data rates of ≈ 200 Gb/s/pol. Results are extracted from the papers cited, or from Fig.4(b).

Symbol rate [Gbd]	Modulation	BER threshold	Required OSNR [dB]	Source
60	DMT	1.7×10^{-2}	36	[18]
64	16-QAM	1×10^{-2}	32	[19]
60	16-QAM	1×10^{-2}	**27**	**this paper**
56	16-QAM	4.5×10^{-3}	28.5	[21]
56	16-QAM	4.5×10^{-3}	**28.5**	**this paper**

By removing the requirement for Kramers-Kronig receiver DSP, we use a DSP flow of the sort commonly used with intradyne receivers. This indicates that the use of a strong LO may enable the reuse of (at least part of) ASIC designs developed for long-haul communications. The receiver hardware design for the system we show here is identical to that used for polarization multiplexed Kramers-Kronig receivers [20, 21], and so requires the same photodiode and ADC bandwidth specifications. So, introducing a relatively strong LO to provide a high CSPR may provide a simpler path to implementation than including a new DSP routine with a much higher required oversampling rate than standard intradyne DSP [17].

If it is then accepted that it is beneficial to include a LO in transceivers, then there arises the question of whether an intradyne receiver is practical. While path length matching may be a costly precision engineering issue if discrete components are used in an optical front end, this is easier to achieve if the receiver is monolithically integrated on a photonic chip-based platform (e.g. [32–34]). Such monolithically integrated devices be useful in short-haul communications if they became widely available and mass-manufactured to reduce per-unit costs. The use of intradyne receivers would then allow the use of lower bandwidth ADCs for the same optical symbol rate compared with heterodyne reception, and so may ultimately have compelling implementation advantages. However, the above argument relies on significant take-up of monolithic receivers by industrial manufacturers. In comparison, the scheme showed here uses existing off-the-shelf components, and so may have greater potential to translate to practical use in the short term.

Optics EXPRESS

6. Conclusion

The inclusion of a LO for single-photodiode coherent detection enables the mitigation of SSBI, where the LO power is high enough to enable a large CSPR. Here we note that a CSPR of 25 dB is sufficient to enable detection of 400Gb/s-class signals. The use of a strong LO allows for lower received OSNRs than for state-of-the-art single-sideband, single-photodiode systems employing a virtual carrier, and removes the need for expanded digital signal processing in receivers to remove SSBI. We show detection of 400Gb/s channels after 150-km transmission in a single-span link, and show that this system can be implemented in installed fiber networks in a field trial test. This work shows that the use of a LO laser in a simplified optical front end may be a beneficial addition to receivers for short-haul, high data rate optical communication systems.

Funding

Australian Research Council (ARC) (CE110001018, FL130100041).

Acknowledgments

We gratefully acknowledge access to dark fibers in AARNet's Melbourne metropolitan network as part of the ALIRT project.